Cellulose (2015) 22:763–778
DOI 10.1007/s10570-014-0524-8

ORIGINAL PAPER

Cytocompatibility and immunomodulatory properties of wood based nanofibrillated cellulose

Miodrag Čolić · Dušan Mihajlović · Aji Mathew · Narges Naseri · Vanja Kokol

Received: 15 September 2014 / Accepted: 8 December 2014 / Published online: 12 December 2014

Abstract Cellulose nanofibrils (CNFs), unique and promising natural materials have gained significant attention recently for biomedical applications, due to their special biomechanical characteristics, surface chemistry, good biocompatibility and low toxicity. However, their long bio-persistence in the organism may provoke immune reactions and this aspect of CNFs has not been studied to date. Therefore, the aim of this work was to examine and compare the cytocompatibility and immunomodulatory properties of CNFs in vitro. CNFs (diameters of 10–70 nm; lengths of a few microns) were prepared from Norway spruce (*Picea abies*) by mechanical fibrillation and high pressure homogenisation. L929 cells, rat thymocytes or human peripheral blood mononuclear cells (PBMNCs) were cultivated with CNFs. None of the six concentrations of CNFs (31.25 μg/ml–1 mg/ml) induced cytotoxicity and oxidative stress in the L929 cells, nor induced necrosis and apoptosis of thymocytes and PBMNCs. Higher concentrations (250 μg/ml–1 mg/ml) slightly inhibited the metabolic activities of the L929 cells as a consequence of inhibited proliferation. The same concentrations of CNFs suppressed the proliferation of PBMNCs to phytohemaglutinine, a T-cell mitogen, and the process was followed by down-regulation of interleukin-2 (IL-2) and interferon-γ production. The highest concentration of CNFs inhibited IL-17A, but increased IL-10 and IL-6 production. The secretion of pro-inflammatory cytokines, IL-1β and tumor necrosis factor-α as well as Th2 cytokine (IL-4), remained unaltered. In conclusion, the results suggest that these CNFs are cytocompatible nanomaterial, according to current ISO criteria, with non-inflammatory and non-immunogenic properties. Higher concentrations seem to be tolerogenic to the immune system, a characteristic very desirable for implantable biomaterials.

Keywords Nanocellulose · Cytotoxicity · T-cell proliferation · Cytokine production · Oxidative stress

M. Čolić (✉) · D. Mihajlović
Medical Faculty of the Military Medical Academy, University of Defense in Belgrade, Crnotravska 17, 11002 Belgrade, Serbia
e-mail: fakultet.vma@mod.gov.rs; mjcolic@eunet.rs

M. Čolić
Medical Faculty, University of Niš, Niš, Serbia

A. Mathew · N. Naseri
Division of Materials Science, Luleå University of Technology, 97187 Luleå, Sweden

V. Kokol
Faculty of Mechanical Engineering, Institute for Engineering Materials and Design, University of Maribor, Maribor, Slovenia

Introduction

Nanofibrillated cellulose or cellulose nanofibrils (CNFs) with diameters within the nanoscale range and length of a few micrometers consists of alternating

crystalline and amorphous domains of longitudinally-oriented cellulose molecules. These molecules are composed of β-1-4-glycosidically-linked anhydroglucose units bearing three reactive hydroxyl groups, thus creating a hydrophilic hydration shell around the particles in an aqueous medium. As such, CNFs have gained increasing attention recently due to their comparatively low cost, high strength and stiffness, combined with high aspect ratios, low weight, biodegradability and renewability, and their tendencies to form colloidal liquid suspension. Such properties offer numerous application opportunities in technical (as reinforcing fillers in composites), food and pharmaceuticals (as additives and binders) or biomedical (tissue engineering, cell therapy, diagnostics, carriers and drug-delivering materials) sectors (Kalia et al. 2013; Habibi 2014; Lin and Dufresne 2014).

CNFs have been investigated as a promising substrate for regenerative medicine and wound healing such as scaffolds for tissue-engineered meniscus, blood vessels, and ligament or tendon substitutes (Mathew et al. 2011, 2012; Jia et al. 2013; Mathew et al. 2013; Lin and Dufresne 2014). The applicability of CNFs as hemodialysis membranes (Ferraz et al. 2012, 2013), antimicrobial nanomaterials (Martins et al. 2012; Liu et al. 2014) and in the pharmaceutical industry as films for long-lasting sustained drug delivery (Valo et al. 2011; Kolakovic et al. 2012) has also been documented. In addition, the native CNF's hydrogel can be used as potential cell culture scaffolds because it provides the desired 3D environments for the growth and differentiation of human hepatic cell lines (Bhattacharya et al. 2012), as well as human pluripotent stem cells (Lou et al. 2014).

As commercial applications have approached, questions have arisen about the safety and biocompatibility of CNFs. Based on a few papers on the biocompatibility of CNFs, it can be hypothesised that this is a safe and biocompatible material (Lin and Dufresne 2014). The first studies showed evidence that highly crystalline regenerated cellulose did not induce the immunological response in vivo in a canine model, as judged by the absence of foreign body reaction (Miyamoto et al. 1989). These results were in accordance with in vitro studies showing that CNFs did not induce toxicity of mouse and human fibroblasts (Mathew et al. 2012; Alexandrescu et al. 2013; Hua et al. 2014), mouse and human macrophages (Vartiainen et al. 2011), human monocytic leukaemia cells (Kollar et al. 2011) and human cervix carcinoma cells (Pitkänen et al. 2014). Recently, in contrast, it seems that cellulose nanocrystals (CNCs) thinner and much shorter than CNFs, might be even toxic and pro-inflammatory, after pulmonary exposition in vivo, as judged by the accumulation of inflammatory cells within the bronchoalveolar fluid and increased production of pro-inflammatory cytokines and chemokines (Yanamala et al. 2014). Such a phenomenon for CNCs was confirmed in a model of 3D human lung cell culture in vitro. However, the cytotoxic and inflammatory effect was slight, perhaps because the applied concentrations of CNCs were low (5–30 μg/ml) (Clift et al. 2011). Under different experimental conditions, by using similar concentrations of CNCs (up to 50 μg/ml, during 48 h of cultivation), Dong et al. (2012) did not show their cytotoxicity against nine different cell lines. A clear dose-dependent cytotoxic effect of CNCs has been reported recently by Pereira et al. (2013). They showed that needle-like CNCs, prepared by acid hydrolysis of cotton cellulose fibers, at very high concentrations (2 mg–5 mg/ml), decreased the viability of bovine fibroblasts in vitro and up-regulated the expression of stress- and apoptosis-related molecules. However, lower concentrations (up to 100 μg/ml) did not influence on cellular viability.

It is obvious that cytotoxicity, as a key parameter of nanocellulose biocompatibility depends on its nanostructural properties, applied concentrations, study models, cell types and exposure times, but many other factors may influence this process such as shape, surface area, charge, source of nanocellulose and the mode of its preparation, degree of agglomeration in culture media, examined biological parameters and assays (Dugan et al. 2013; Kalia et al. 2013; Habibi 2014; Lin and Dufresne 2014). Moreover, biocompatibility is not the only parameter to be investigated before the clinical applications of biomaterials. Within this context, the response of the immune system, as a key protective component of the organism, is of particular importance, as cellulose fibrils have lengthy bio-persistence in the body and thus may provoke immune reactions (Tatrai et al. 1996; Muhle et al. 1997; Dugan et al. 2013; Lin and Dufresne 2014).

To date, almost nothing is known about the adaptive immune responses of any type of nanocellulose, particularly wood-derived CNFs. Therefore, the aim of our study was to examine the cytocompatibility of CNFs using two different cell lines, by

screening cell death, mitochondrial activity, oxidative stress and proliferation, as well as their capabilities to modulate the immune response using an in vitro model of human mitogen-activated peripheral blood mononuclear cells (PBMNCs).

Materials and methods

Preparation and characterisation of CNFs

Bleached dissolving cellulose (also called dissolving pulp) from Norway spruce (*Picea abies*) with very high (95 %) cellulose content and (4.75 %) hemicellulose and low lignin content was supplied by Domsjo Fabriker AB, Sweden, and used as starting material. Cellulose fibres were dispersed in distilled water at a 2 wt% concentration suspension by using the Silverson L4RT mechanical blender (England) at 6,000 rpm for 15 min. CNFs were then isolated by mechanical fibrillation using an ultrafine grinder (MKCA 6–3 from Masuko, Japan) at 1,440 rpm for 30 min, followed by a high pressure homogeniser (Model 2000, APV, Denmark) as described in Jonoobi et al. (2014). The chemical composition of the CNFs obtained was considered to be same as the raw material as no chemical treatments were carried out during the fibrillation process. The CNFs' suspensions were stored in a refrigerator until further use.

Produced CNFs were evaluated by atomic force microscopy (AFM) (Nanoscope V, Veeco, USA). The cellulose suspensions were diluted with water and dried on a freshly cleaved mica plate. The equipment was operated in tapping mode using etched silicon probes (FESP, Veeco, USA) at a resonance frequency of about70 kHz and a spring constant of 1–5 N/m.

The ζ-potential and average size measurements of the CNFs were performed in a 0.01 M phosphate buffered saline (PBS of Sigma-Aldrich powder P3813, containing 0.138 M NaCl and 0.0027 M KCl) solution at pH 7.4 by a Nano ZS ZEN 3600, Malvern instruments Ltd., UK, using the laser of 633 nm and a field of 40 V across the nominal electrode spacing of 16 mm. All measurements were carried out at 25 ± 1 °C using the refractive index (1.33 vs. 1.48) and viscosity (0.8872 vs. 1.48 cP) of water versus cellulose for data analysis, being performed with Malvern Zetasizer Software 7.02. Each measurement was comprised of at least three runs. The influence of CNFs concentration and sonication conditions (time and amplitude) of dispersions on the ζ-potential and average size was preliminary evaluated in order to ascertain the relevance and validity of the data. Finally, the samples being prepared as 0.05 % w/v solutions in PBS and additionally diluted to 0.005 % w/v with Milli-Q water, were sonicated for 2 min at 25 % amplitude before ζ-potential analysis using a SONICS Vibra cell™ VCX 750 ultrasonic processor, Sonics & Materials, Inc., USA. The measurements were done in triplicate and the average data reported. The ζ-potential of the CNFs with average size of 33,165 ± 2,516 nm in PBS was estimated to be −23.84 ± 6.54 mV, being attributed to partly dissociated terminal-located carboxylic ($-COO^-$) acid groups.

Preparation of CNFs for cell cultures

The starting preparation of CNFs was 2 % solution in deionized water (20 mg/ml). Before the experiment, the samples of CNFs were sterilized in an autoclave at 121 °C during 20 min and then sonicated in an ultrasonic bath for 10 min. The concentrations used in the cell cultures ranged from 31.25 μg/ml to 1 mg/ml, and were prepared in a complete RPMI medium consisting of a basic RPMI 1640 medium (Sigma, Munich, Germany) supplemented with 2 mM L-glutamine (Sigma), 20 μg/ml gentamicin, 100 U/ml penicillin, 100 mg/ml streptomycin (all antibiotics from ICN, Costa Mesa, CA, USA), 50 μM 2-mercaptoethanol (Sigma), and 10 % heat inactivated fetal calf serum (FCS), (PAA Laboratories Vienna, Austria). The level of endotoxin in the highest concentration of CNFs, as determined by the Limulus Amebocyte Lysate (LAL) test was 0.32 EU/ml.

In order to assess the morphology, fresh suspensions of CNFs (250 μg/ml) or suspensions of CNFs cultivated in a complete culture medium for 24 h, were centrifuged onto glass microscopic slides using a cytocentrifuge (Thermo Fisher Scientific Inc., MA, USA). After drying, the glass slides were stained with Calcofluor white (Sigma) according to the manufacturer's protocol and analyzed with an epifluorescence microscope (Nikon Eclipse 5i equipped with a Nikon DXM1200C Camera, Tokyo, Japan) using UV-2A filter (EX 330-380, DM 400, BA 420).

L929 cells

L929 cells, an immortalized fibroblast cell-line, were obtained from ATCC (Rockwell, MD, USA) and kept in liquid nitrogen. After defrosting, the cells were propagated in the complete RPMI medium.

Morphological analysis

L929 cells (1×10^4 cell/well) were incubated in the complete RPMI medium in 24-well plates (Sarstedt, Nümbrecht, Germany) with different concentrations of CNFs (31.25 μg/ml–1 mg/ml). The cells without CNFs served as negative controls, whereas L929 cells treated with 1 % Triton X-100 (Sigma) were positive controls. After 48 h, the following morphological characteristics were analyzed by an inverted light microscope (IX51; Olympus, Tokyo, Japan): shape, proliferation rate, attachment to plastic, vacuolization of the cytoplasm, signs of cell death.

Viability and apoptosis

After morphological analysis, the cells, cultivated with six different concentrations of CNFs (31.25 μg/ml–1 mg/ml) or without CNFs, were washed twice with PBS and detached from the plastic by using 0.25 % trypsin in PBS. The viability was determined by staining the cells with propidium iodide (PI) (Sigma) 20 μg/ml in PBS. The analysis was done within 5 min by using a cytofluorometer (CyFlow Cube 6, Partec GmbH, Münster, Germany). PI^+ cells were considered as necrotic cells. The percentage of viable cells was determined by subtracting the percentage of necrotic cells from 100 %.

Apoptosis was determined by staining L929 cells, in suspension with PI (50 μg/mL dissolved in a hypotonic citric/Triton-X buffer) using flow cytometry as described for necrosis assay. The cells with hypodiploid nuclei (sub-G0 pick) represented apoptotic cells. At least 5,000 cells were analyzed and the results are expressed as mean percentage of apoptotic cells from triplicate measurements.

MTT asay

L929 cells, seeded in 96-well plates (Sarstedt) (0.5×10^4 cells/well, in triplicates), were incubated for 24 h before the test in 100 μl of complete RPMI medium. Then the medium was removed and 200 μl of CNF suspensions (31.25 μg/ml–1 mg/ml) were added, followed by centrifugation of the plates (500 g, 10 min) to allow better contact of the nanomaterials with the adherent cells. The L929 cells were cultivated for 48 h in an incubator with 5 % CO_2 at 37 °C. The wells with L929 cells, cultivated in medium alone, served as negative controls, whereas the wells treated with 1 % Triton X-100 (Sigma) during the final 2 h were positive controls.

The metabolic activity of the L929 cells was determined by a colorimetric assay (Tada et al. 1986). At first, the supernatants of the cells' cultures were removed and solutions of 3-[4,5 dimethyl-thiazol-2lyl]-2.5 diphenyl tetrazolium bromide (MTT) (Sigma) (100 μl/well, final concentration 500 μg/ml), were added to each well. Wells with an MTT solution without the cells served as blank controls. The additional controls were those wells with different concentrations of CNFs without cells. The wells were incubated with MTT for 4 h in an incubator at 37 °C with 5 % CO_2. Then 100 μl 0.01 N HCl/10 % sodiumdodecyl-sulphate (SDS) (Merck, Darmstadt, Germany) was added to each of the 96-wells to dissolve formazan overnight. The next day the plates were centrifuged at 800 g for 10 min in order to pellet any remaining CNFs. After that, the supernatants were transferred to new plates and the optical density (OD) of the developed color was read at 570 nm (ELISA reader, Behring II). The results were expressed as the relative metabolic activity compared to the corresponding negative controls.

$$\text{Metabolic activity} = ((\text{OD of cells cultivated with CNFs} - \text{OD of corresponding CNFs cultivated without cells})/(\text{OD of cells cultivated without CNFs} - \text{OD of control medium cultivated without cells})) \times 100.$$

Detection of reactive oxygen species

CNFs (250 μg/ml–1 mg/ml) were added to the monolayer of L929 cells, which were seeded in 24 well plates (Sarstedt) (5×10^4/well) 1 day before the test, and the cultures were incubated for an additional 48 h. The cells treated with $CuCl_2$ (50 μM; Sigma) in complete RPMI medium for 1 h were used as a positive control. In order to assess oxidative stress, the monolayers of L929 cells

were washed carefully twice with PBS, to remove loosely adherent CNFs. The cells were then collected by trypsinisation, washed in Hanks' Balanced Salt solution (HBSS), and incubated subsequently with dihydrorhodamine 123 (DHR123; 25 μM; Invitrogen Carlsbad, CA, USA) in a HBSS buffer for 20 min at room temperature. Then the cells were fixed with 0.5 % paraphormaldehyde and analysed by flow cytometry (CyFlow Cube 6, Partec) within 1 h.

Determination of glutathione (GSH) and lactate dehydrogenase (LDH)

L929 cells (5×10^4cell/well) were incubated for 24 h in complete RPMI medium in 24-well plates (Sarstedt). Afterwards, the medium was removed carefully and the cells were treated with different concentrations of CNFs (31.25 μg/ml–1 mg/ml). The cells treated with 1 % Triton X-100 (Sigma) during the last 2 h were positive controls. After 48 h, supernatants were removed, centrifuged at 800 g for 10 min to remove any remaining CNFs and then analysed for LDH activity, using a LDH kit (Bayer Diagnostics Corporation) adapted to the auto analyser (ADVIA 1800, Siemens AG, Erlangen, Germany). L929 cells were washed carefully twice with PBS to remove CNFs, harvested by trypsinisation, washed, counted and used in the GSH assay. LDH activity was normalized to the equal number of L929 cells (1×10^4).

The GSH levels were measured by an enzymatic recycling method described in detail by Rahman et al. (2007). This assay is based on the reaction of GSH with 5,5-Dithiobis (2-nitrobenzoic acid) (DTNB) that forms the yellow derivative 5´-thio-2-nitrobenzoic acid (TNB). The rate of TNB formation is directly proportional to the concentration of GSH. The optical density changes were measured at 405 nm using a Synergy HT multi-modal plate reader (Bio-Tec Instruments, Inc., Winooski, VT). The values were expressed as percentages of GSH activity relative to the control used as 100 %.

Proliferation assay

L929 cells (3×10^4/well of 24-well plate (Sarstedt)) were plated with different concentrations of CNFs (31.25 μg/ml–1 mg/ml) or without CNFs (control) for 48 h in an incubator with 5 % CO_2. The cultures were pulsed with [^{3}H]-thymidine for the last 8 h (1 μCi/well, Amersham, Buckinghamshire, UK). Before harvesting, the cells were detached from the wells by treatment with 0.25 % trypsin in PBS for 10 min. Radioactivity was measured by using a Beckman scintillation counter and expressed as counts per minute (cpm) of triplicates. The values were expressed as relative proliferation (%) compared to control (L929 cells without CNFs) used as 100 %.

Thymocytes

Thymocytes were prepared from thymuses of Albino Oxford (AO) rats, 10 weeks old. These rodents were bred in a Vivarium of the Institute for Medical Research, Military Medical Academy (MMA), Belgrade, Serbia, under standard conditions and their use for the experiments was in accordance with the European Community Guidelines for the Use of Experimental Animals (Directive 2010/63/EU), approved by the Ethical Committee of the MMA. The rats were killed using ether and their thymuses removed aseptically and placed in Petri dishes. The thymocytes were released by pressing the thymus with a syringe plague, followed by filtration of the cellular suspension using a pre-separation filter with a pore size of 30 μm. The viability of the thymocytes as determined by 1 % of Trypan blue staining, was higher than 95 %.

Apoptosis assays

The thymocytes were seeded in 96-well plates (Sarstedt) (1×10^6 cells/well) and cultivated in 200 μl of complete RPMI medium with different concentrations of CNFs (31.25 μg/ml–1 mg/ml) or without CNFs (control medium alone) for 24 h. After that apoptosis was assessed using a morphological method after staining of the cells with 0.5 % Türk solution (Colic et al. 2000) or by Annexin-V-FTIC/PI kit (Invitrogen) followed by flow cytometry analysis.

For morphological evaluation of apoptosis 10 μl cell suspension was mixed with 30 μl Türk solution. The solution fixes and stains the nuclei, enabling a clear distinction between the chromatin structure in viable and apoptotic cells. Cells were analyzed using a light microscope (Olympus) and thymocytes with condensed chromatin or fragmented condensed nuclei were considered as apoptotic cells. At least 500 cells were examined in each sample and the results are expressed as percentages.

The flow cytometric method was performed exactly by instructions of the manufacturer. This test enables identification of early apoptotic (Annexin-V-FITC$^+$/PI$^-$) cells, late apoptotic/ secondary necrotic (Annexin-V-FITC$^+$/PI$^+$) cells, and primary necrotic (Annexin-V-FITC$^-$/PI$^+$) cells.

Peripheral blood mononuclear cells

The PBMNCs were obtained from the buffy coats of 6 healthy volunteers upon obtaining a signed informed consent. Buffy coat was diluted 3 times with PBS and carefully layered on density gradient (Lymphoprep, PAA). After centrifugation (1000 g, 20 min) at room temperature, the interface layer consisting of mononuclear cells was collected. Cells were washed four times by low-speed centrifugation (130 g, 8 min) with PBS at room temperature in order to remove remaining platelets. Finally, the cells were resuspended in complete RPMI medium and cell number as well as viability was assessed under a light microscope (Olimpus) using Trypan blue staining. The PBMNCs were afterwards used in cell culture assays.

[^{3}H]-thymidine uptake assay

Human PBMNCs (3×10^5/well of 96-well plate (Sarstedt)) ($n = 6$) were stimulated with phytohemagglutinin (PHA) (32 μg/ml) alone or PHA with different concentrations of CNFs (31.25 μg/ml–1 mg/ml) for 72 h in an incubator with 5 % CO_2. The cultures were pulsed with [^{3}H]-thymidine for the last 18 h (1 μCi/well, Amersham). At the end of the cultivation period the cells were harvested and the radioactivity (expressed as cpm) was counted using a Beckman scintillation counter. The values were expressed as relative proliferation (%) compared to control (PHA-stimulated cells without CNFs) used as 100 %. Parallel cultures were setup for the detection of cytokines in culture supernatants after 48 h of cultivation. The supernatants were collected, centrifuged and frozen until cytokine analysis was done, whereas the cells were counted by light microscopy.

Apoptosis and necrosis

PHA stimulated PBMNC cultures, cultivated as described above, were collected and washed twice by low-speed centrifugation (130 g, 8 min) to remove CNFs remaining in the supernatant. After that, the cells were counted and stained with either PI in PBS (as described for L929 necrosis assay) or PI in hypotonic citrate buffer (as described for L929 apoptosis assay). Flow cytometric analysis was performed on CyFlow Cube 6 (Partec) analyzer (5,000 cells were analyzed per sample).

Detection of cytokines

The levels of IL-1β, IL-2, IL-6, IL-4, IL-10, IL-17A, TNF-α and IFN-γ were determined in supernatants of PHA-stimulated PBMCs cultures. The levels of cytokines were determined using the commercial sandwich ELISA kits (R&D System), according to the manufacturer's protocol. The unknown concentrations of cytokines were calculated from the standard curve obtained with known concentrations of corresponding cytokines. The values of cytokines were additionally normalized to the equal number (1×10^5) of cells.

Statistical analysis

The results are presented as the mean ± standard deviation (SD) of 3–6 independent experiments as indicated in Figure legends. The parametric tests were used to evaluate the differences between the experimental and corresponding control samples, if the data followed Gaussian distribution. Otherwise non-parametric tests were carried out. Values at $p < 0.05$ or less were considered significant statistically. All statistical analysis was performed in Graph Pad Prism 5 software (La Jolla, CA, USA).

Results

Characterisations of CNFs

The AFM height image, amplitude image and the measurement of diameters from height image (Fig. 1) showed CNFs that were well separated or partially separated ones, as well as those regions where the nanofibrils were even bundled together. Therefore the typical diameters of the nanofibrils measured from well isolated regions had a diameter of 10–35 nm, whereas some aggregated nanofibrils with diameters as high as 70 nm were also found. The study showed

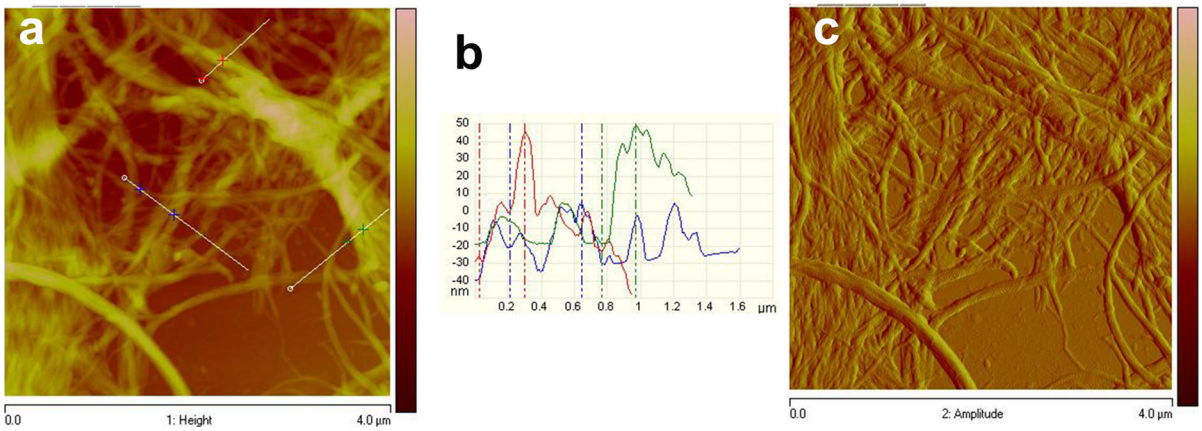

Fig. 1 The AFM height image (**a**), the measurement of diameters from height image (**b**) and amplitude image (**c**) of CNFs

that the isolated material has two-dimensional nano-entities with the diameter in nanoscale and the lengths in micron scale (>10 µm).

In order to assess the behavior of CNFs in the complete RPMI medium, CNF suspensions were centrifuged onto microscopic slides before and after cultivation in the culture medium for 24 h and the spins were stained with Calcofluor white. The analysis by fluorescence microscopy showed that, except for the presence of fine fibrils, different in lengths, and the fibro-reticular structures, the samples consisted of clumped fibrils and cellulose aggregates, different in sizes and irregularly shaped. These characteristics also well correlated with the ζ-size measurements. No significant differences in morphology were seen between the freshly prepared and cultivated CNFs (Fig. 2).

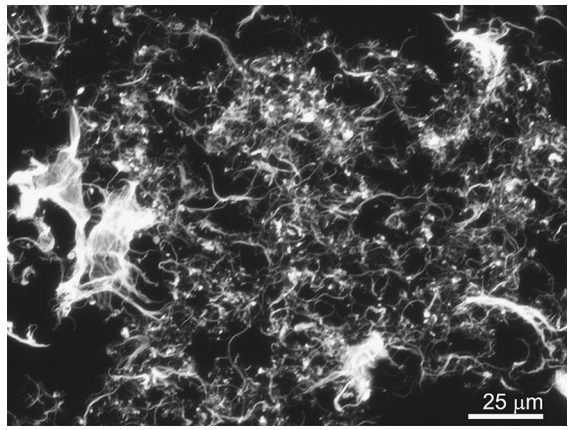

Fig. 2 Fluorescent microscopic analysis of CNFs. CNFs' spins were stained with Calcofluor white and analysed by an epi-fluorescent microscope under UV excitation 330-385 nm. Note fine fibrillar structures, but also larger and smaller aggregates of CNFs

Cytocompatibility of CNFs

The cytocompatibility of CNFs was studied by cultivating different concentrations of CNFs with L929 cells. After an incubation time (48 h), the cultures were analysed by inverted light microscopy (Olympus). The control L929 cells almost reached confluence and some of them showed mitotic activity (Fig. 3a). The culture of L929 cells with CNFs showed intact cell morphology without signs of cytopathic effect (degeneration, vacuolization of cytoplasm, detachment from the plastic or morphological signs of cell death) (Fig. 3b), which were clearly visible in positive control cultures (Fig. 3c). However, in cultures with higher concentrations of CNFs, (250 µg/ml–1 mg/ml), of which the highest one covered the L929 monolayers almost completely, a reduced number of cells was detected (Fig. 3b). The microscopic examination demonstrated that mostly fine, reticular structures of CNFs were attached to the L929 cells, whereas mostly aggregated and bundled CNFs floated within the medium above the cells.

The MTT assay confirmed that the L929 cells, cultivated with higher concentrations of CNFs showed a dose-dependent decrease in the metabolic activity (Fig. 3d). The inhibition of MTT activity with the highest concentration of CNFs was 24.2 ± 6.4 %. The process was not associated with cell death, as concluded by the absence of LDH

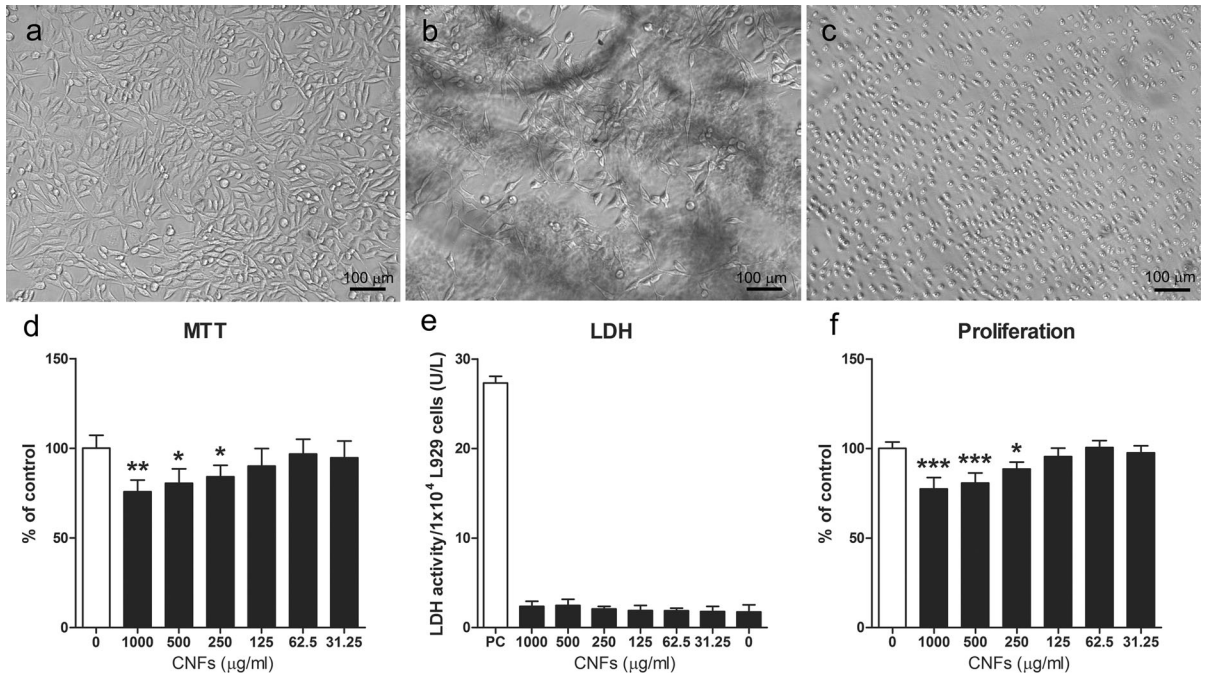

Fig. 3 Cytocompatibility of CNFs studied on L929 cells. L929 cells were cultivated with different concentrations of CNFs for 48 h. **a** Intact morphology of negative control culture, **b** reduced proliferation of cells in the presence of 500 µg/ml of CNFs, **c** cell death in the presence of Triton X-100 (positive control - PC). **d** MTT assay, **e** LDH assay, **f** [^{3}H]-thymidine uptake assay. Values for MTT and [^{3}H]-thymidine uptake assays are given as percentages of control (mean ± SD; n = 5), whereas results for LDH assay are normalized to equal number of L929 cells (1×10^4) and presented as mean ± SD; n = 4. $*p < 0.05$; $**p < 0.01$; $***p < 0.001$ compared to corresponding controls (L929 cells cultivated alone)

release (Fig. 3e), cell necrosis (0.8 ± 0.4 % necrotic L929 cells using 1 mg/ml of CNFs versus 0.9 ± 0.5 % necrotic cells in control cultures) and apoptosis (1.2 ± 0.2 % apoptotic cells in the presence of 1 mg/ml of CNFs versus 1.1 ± 0.4 % apoptotic cells in control cultures). However, these findings correlated with decreased proliferation of L929 cells, as revealed by [^{3}H]-thymidine incorporation (Fig. 3f). The inhibition of proliferation using the highest concentration of CNFs was 22.6 ± 6.5 %.

In order to see whether inhibition of cellular proliferation in the presence of higher concentrations of CNFs is associated with oxidative stress, we performed colorimetric and flow-cytometric assays. The results presented in Fig. 4 showed that both GSH levels and DHR123 fluorescence in L929 cultures were not altered, even in the presence of the highest (1 mg/ml) concentrations of CNFs.

The cytotoxic assay was extended on rat thymocytes, a type of non-proliferating cells, by measuring apoptosis. Apoptosis of thymocytes was detected by using the morphological method (staining of cells with Türk solution) and by Annexin V-FITC/PI staining assay (flow cytometry). As shown in Fig. 5a, the spontaneous apoptosis of thymocytes was high, but neither concentration of CNFs enhanced apoptosis of thymocytes. Similar results were obtained using flow cytometry (Fig. 5b). As seen neither concentration of CNFs significantly modulate the percentage of early apoptotic (Annexin-V-FITC$^+$/PI$^-$) cells and late apoptotic/secondary necrotic (Annexin-V-FITC$^+$/PI$^+$) cells, nor induced primary necrosis (Annexin-V-FITC$^-$/PI$^+$) of thymocytes.

Immunomodulatory properties of CNFs

The study related to the immunomodulatory properties of CNFs was performed on human PBMNCs stimulated with PHA, a T-cell mitogen. The cells were cultivated for 3 days with different concentrations of CNFs or in a control medium alone and then the proliferation was measured. The results presented

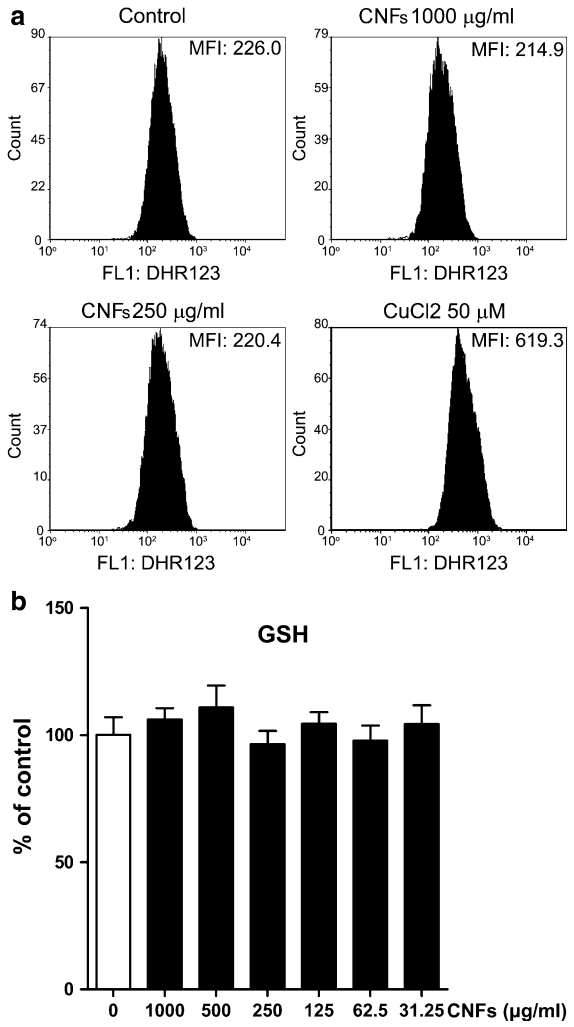

Fig. 4 Effect of CNFs on oxidative stress of L929 cells. L929 cells were incubated in the absence or presence of different concentrations of CNFs for 48 h. The cells treated with $CuCl_2$ (50 μM) for 1 h were used as a positive control. To assess ROS production (**a**), cells were incubated with DHR123 in a HBSS buffer for 20 min, fixed with 0.5 % paraphormaldehyde and analysed by flow cytometry. The results are presented as the representative histograms from three experiments. The numbers represent mean fluorescent intensity. Intracellular GSH levels (**b**) were determined using an enzymatic recycling method based on the reaction of GSH with DTNB. The data are showed as percentages relative to control (mean ± SD, n = 3)

in Fig. 6a show that higher concentrations of CNFs (250 μg/ml–1 mg/ml) inhibited the proliferative response of PBMNCs to PHA in a dose-dependent manner. The anti-proliferative activity of CNFs was not a consequence of their cytotoxicity, as neither the percentage of apoptotic cells (Fig. 6b) nor the percentage of necrotic cells (Fig. 6c) significantly differed compared to the control cells.

The supernatants of the PHA-stimulated cultures were analysed for the presence of pro-inflammatory cytokines (IL-1β, TNF-α, IL-6). CNFs, at any of the concentrations tested, did not significantly modulate the production of IL-1β (Fig. 7a) and TNF-α (Fig. 7b). The highest concentration of nanocellulose increased the production of IL-6, whereas other concentrations were non-modulatory (Fig. 7c).

The levels of the four main Th cytokines: IFN-γ (Th1), IL-4 (Th2), IL-17A (Th17), IL-10 (T regulatory cytokines; Tregs) and IL-2 (a main T-cell growth factor) were also determined in the supernatants of PHA-stimulated PBMNC cultures. CNFs, at concentrations of 250, 500 μg/ml and 1 mg/ml inhibited the production of IL-2 (Fig. 7d) and IFN-γ (Fig. 7e), dose dependently. The highest concentration of CNFs inhibited the levels of IL-17A (Fig. 7f), whereas the levels of IL-4 (Fig. 7g) and IL-10 (Fig. 7h) were not significantly changed. A similar modulatory effect of CNFs on cytokine levels was observed when the levels of cytokines were normalised to equal numbers ($1x10^5$) of cells in the cultures. An exception was the elevated level of IL-10 in the presence of the highest concentration of CNFs.

Discussion

In this paper, we studied the cytocompatibility and immunomodulatory properties of CNFs using different in vitro cell models. The cytotoxicity studies demonstrated that CNFs, even at high concentrations, (1 mg/ml), were not toxic for L929 cells, rat thymocytes, and human PBMNCs, as neither cell death nor significant oxidative stress were induced. However, a significant down-modulatory effect on T-cell functions was observed and this is the first report about the capabilities of CNFs to modulate the adaptive immune response.

The initial cytocompatibility study was performed on a permanent fibroblast cell line, based on recommendations by ISO10993-5 (2009) for testing the cytotoxic activity of medical devices, including biomaterials. We studied the responses of L929 fibroblastic cells to different concentrations of CNFs, by measuring LDH release, apoptosis and necrosis as signs of cell death, morphological changes of cells in

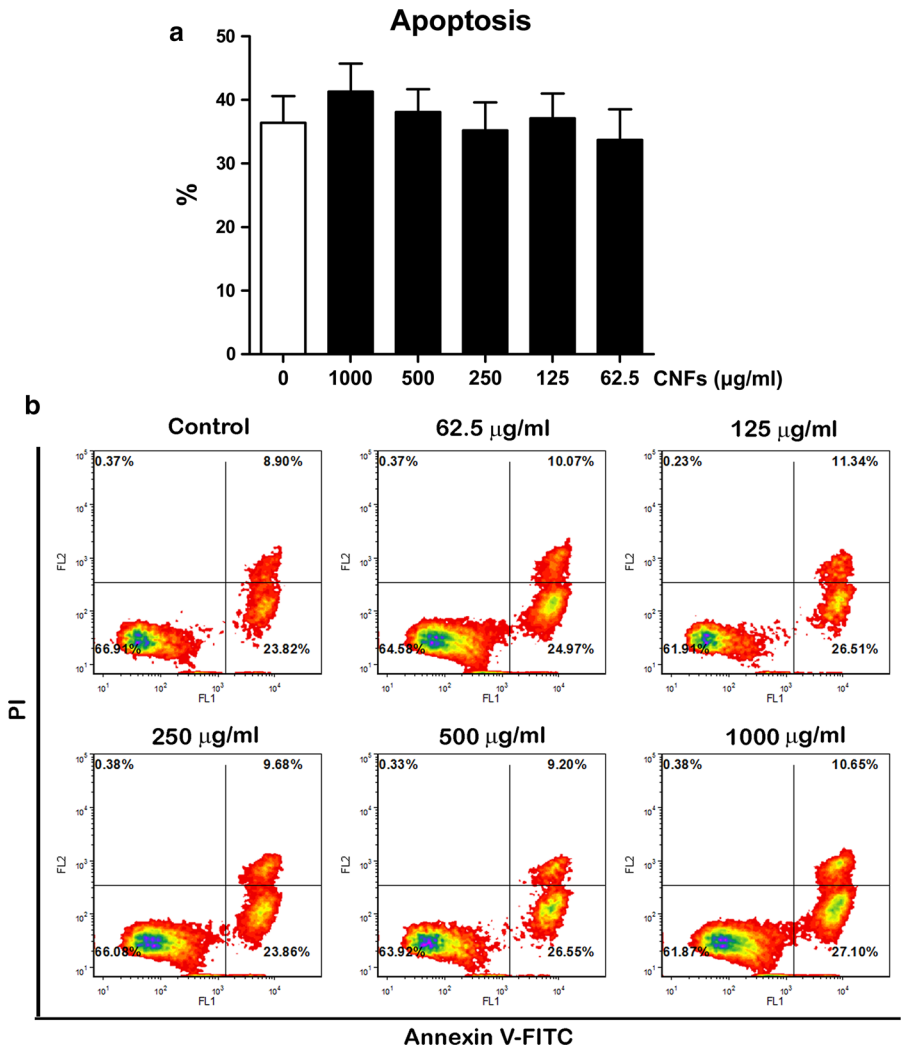

Fig. 5 Effect of CNFs on the apoptosis of rat thymocytes. Thymocytes were cultivated with different concentrations of CNFs or in a control medium, for 24 h. After that, the cells were stained with Türk solution and analyzed by a light microscope. **a** Values are given as percentages of apoptotic cells (mean ± SD, n = 3 different experiments). In addition, cells were stained with Annexin-V-FITC/PI, and analysed by flow cytometry. The representative density plots from one out of three experiments with similar results are presented (**b**)

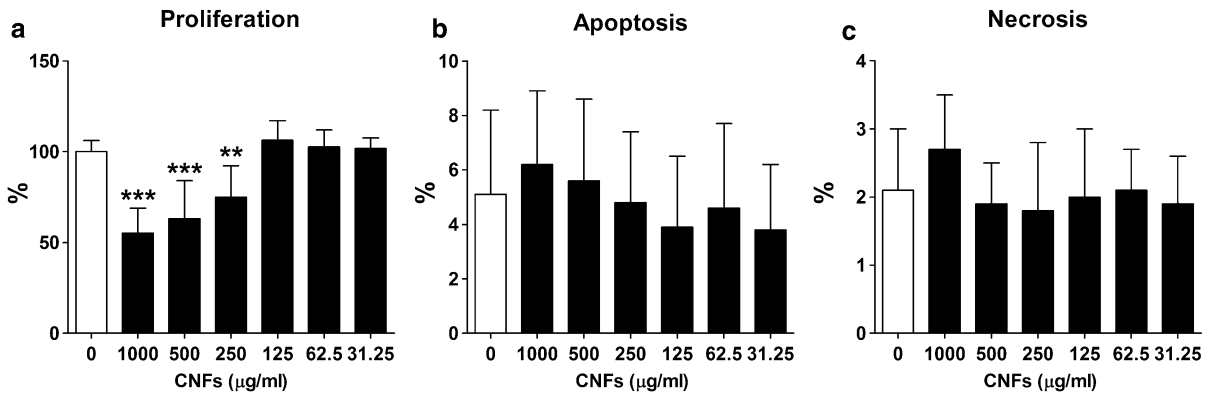

Fig. 6 Effect of CNFs on proliferation, apoptosis and necrosis of human PBMNCs. PBMNCs were cultivated with PHA alone or with PHA in the presence of different concentrations of CNFs. After 72 h, cell proliferation (**a**), apoptosis (**b**) and necrosis (**c**) were determined. Values are given as mean ± SD (n = 6). *$p < 0.05$; **$p < 0.01$; ***$p < 0.001$ compared to corresponding controls

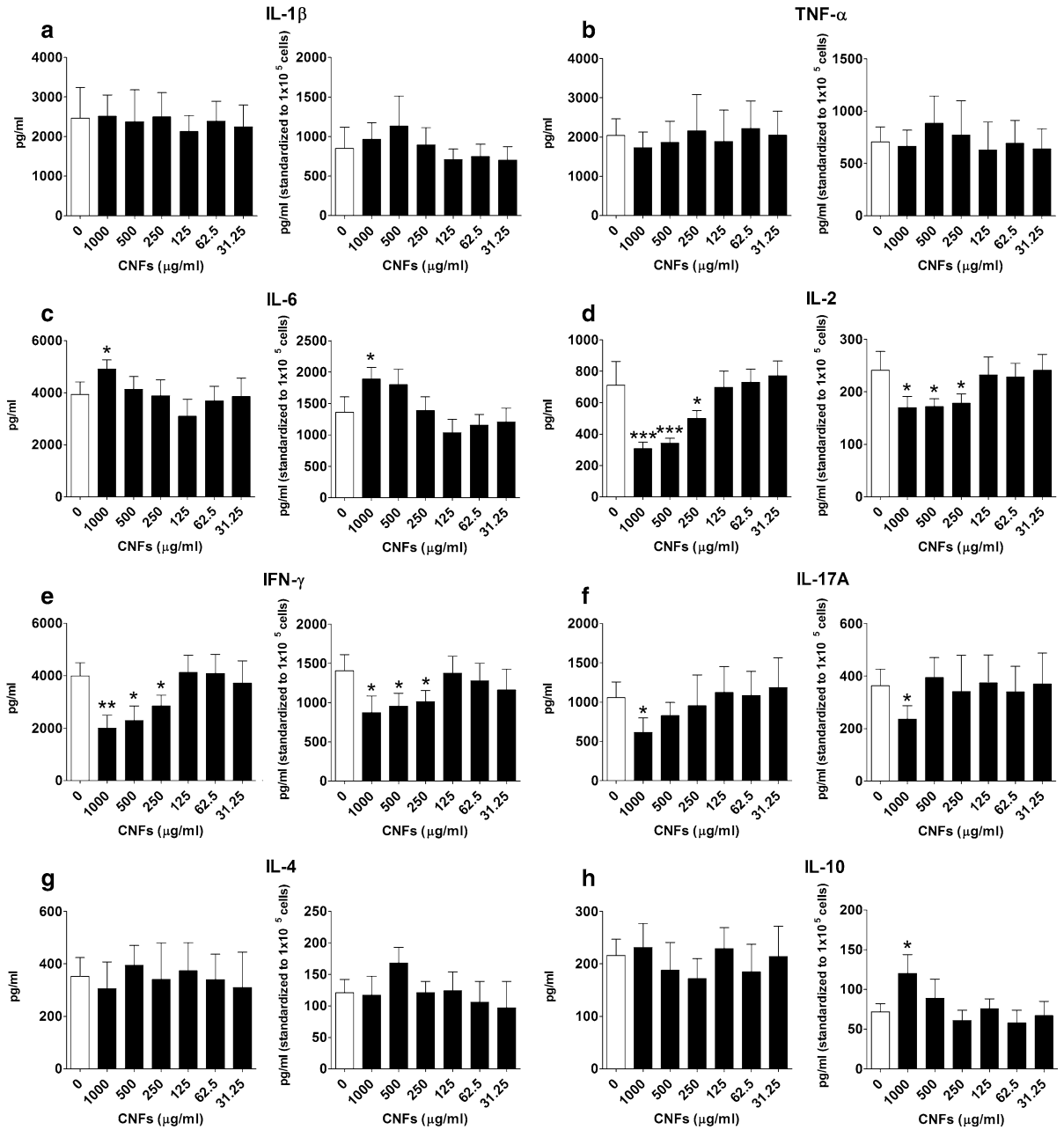

Fig. 7 Effect of CNFs on pro-inflammatory and Th cytokine production in PBMNCs cultures. PBMNCs were stimulated with PHA alone or with different concentrations of CNFs for 72 h. The levels of pro-inflammatory cytokines: IL-1β (**a**), TNF-α (**b**), IL-6 (**c**) and Th cytokines: IL-2 (**d**), IFN-γ (**e**), IL-17A (**f**), IL-4 (**g**), IL-10 (**h**) were measured by ELISA in the culture supernatants. Cytokine concentrations are presented as mean levels ± SD or mean levels ± SD normalized to 1×10^5 cells (n = 3). *$p < 0.05$; **$p < 0.01$; ***$p < 0.001$ compared to corresponding controls

the cultures and their proliferation. The cells cultivated with CNFs had preserved morphology without signs of cell death but at higher concentrations a slight inhibition of cellular proliferation was detected, as judged by decreased metabolic activities of the L929 cells and reduced [^{3}H]-thymidine uptake. The inhibition of cell proliferation with the highest concentration (1 mg/ml), which is very high for

cytocompatibility testing, did not exceed 30 %. The inhibition of metabolic activity proliferation of L929 cells was probably not a consequence of induced oxidative stress as neither the levels of glutathione as an oxidative stress protective molecule (Rahman et al. 2007) nor the increase in DHR-123 fluorescence as an indicator of a generation of intracellular reactive oxygen species (Chen and Junger 2012), were modified by CNFs.

Regarding the toxicity of CNFs, no changes in the cell viability or morphology of human monocytes and mouse macrophages (Vartiainen et al. 2011), as well as human cervix carcinoma (HeLa229) cells (Pitkänen et al. 2014) were observed. In addition, the cytotoxicity of CNFs has been published by Alexandrescu et al. (2013) using mouse 3T3 fibroblasts. The authors used different approaches, also according ISO10993-5 (2009), by examining the viability and morphology of 3T3 cells which were grown on compact samples of CNFs from wood (different preparation of *Eucaliptus* and *Pinus radiata*), in direct contact, as well as the effect of elution extracts from these specimens (indirect contact) on the metabolic activity and proliferation of 3T3 fibroblasts. Both approaches clearly indicated that cell membrane integrity, cell mitochondrial activity, but also the DNA proliferation, remained unchanged during the tests suggesting that these neat cellulose nanostructured materials were not toxic against fibroblasts cells. In another recent study, Hua et al. (2014) investigated cytocompatibility of unmodified, cationized and anionized nanofibrillated cellulose from wood on human dermal fibroblasts using indirect and direct cell tests. In the indirect test, no cytotoxic effects were observed, whereas the direct contact test showed that cationic modified-CNFs demonstrated better cytocompatibility than unmodified and anionic modified-CNFs.

Pereira et al. (2013) have confirmed recently that cotton CNCs, at concentrations between 2 μg/ml - 100 μg/ml, do not cause the death of bovine fibroblasts, whereas those within the ranges between 200 μg/ml – 1 mg/ml are slightly inhibitory, similarly as we found with wood-derived CNFs. Significant cytotoxicity of these CNCs was obtained using very high concentrations (2–5 mg/ml) and this process was associated with increased expressions of stress-related genes, such as heat shock protein 70 and peroxiredoxin-1 as well as the gene coding B-cell leukemia associated X protein, an apoptosis-promoting molecule.

Our results are also comparable to those published by Moreira et al. (2009) who showed that bacterial nanocellulose at concentrations between 100 μg/ml – 1,000 μg/ml reduced the proliferation of 3T3 fibroblasts and CHO cells by about 15–20 % after 72 h of cultivation. They did not observe any difference in cellular morphology, similarly as our microscopic analysis revealed. Slight inhibition of cellular proliferation was documented upon cultivation of cells either on bacterial nanocellulose membranes (Backdahl et al. 2006) or on nanocomposites prepared by partial dissolution of CNFs (Mathew et al. 2012). It is interesting that the liquid extract prepared by conditioning a nanocomposite consisting of CNFs and collagen fibrils, did not induce cytotoxicity of the 3T3 cells. However, when used as a solid substrate, the nanocomposite slowed-down the proliferation of human ligament and endothelial cells initially, but supported the cellular proliferation afterwards (Mathew et al. 2013).

Although, according to ISO10993-5 (2009), inhibited proliferation up to 30 %, as was the case in our study, is not considered as a cytotoxic phenomenon and such a material is classified as biocompatible, the results may be interpreted with caution. The reason for inhibited cellular proliferation in the presence of CNFs is hard to explain but further research should be focused on the specific surface chemistry, especially on the protein exchanges on the surfaces of the CNFs because such properties significantly affect the interactions of different nanoparticles with mammalian cells (Monopoli et al. 2011). In addition, high concentrations of CNFs used in the cultivation assay with adherent cells may disturb cell growth by their physical properties. The aggregation of CNFs in cell culture media and its kinetics may also influence the results, therefore real effective concentrations of CNFs are difficult to measure. One way to remove aggregates is fractionation as reported by Pitkänen et al. (2014). They showed that smallest fractions of CNFs are not cytotoxic for adherent HeLa229 cells, but their behavior in adherent and potentially in cell suspension cultures should be further investigated.

Proliferating cells are not always suitable for cytotoxicity studies, especially when the toxic potential of the examined materials is very low. Therefore, we used rat thymocytes as a type of non-

proliferating lymphocytes. These cells were chosen based on our previous publication about their higher sensitivity to the toxic effect of smart materials than L929 cells (Čolić et al. 2010). Thymocytes rapidly die in cultures by apoptosis and the process is significantly enhanced by different noxious stimuli (Deng et al. 1999). However, our results clearly showed that even at the highest dose, apoptosis of thymocytes did not significantly differ from the negative control. CNFs did not induce necrosis of thymocytes, too. Cumulatively, these and previous results on L929 cells, according to ISO10993-5 (2009) classification of cytotoxicity, suggest that CNFs, even at high concentrations (1 mg/ml) are a cytocompatible nanomaterial.

The most significant part of our results concerned the effects of CNFs on T-cell functions in a model of human PBMNCs stimulated with PHA. It is known that PHA is a T-cell mitogen, which stimulates the proliferation of T-cells in the presence of accessory cells, predominantly monocytes and blood dendritic cells. By cross-linking T-cell receptor and various activating molecules on T-cells and accessory cells, PHA provides necessary receptor-transmitted signals and those mediated by soluble cytokines, thus allowing transcription of key factors for T-cell growth (O'Flynn et al. 1985; Mihajlovic et al. 2014). We demonstrated that CNFs at higher concentrations, inhibited the T-cell proliferation and the suppressive effect with the highest concentration was about 40 %. The inhibition of T-cell proliferation is an immunological phenomenon, not related to cell death, but associated with a significant decrease in IL-2 production. It can be hypothesized that suppressed proliferation of T-cells was due to lower production of IL-2, because this cytokine is a crucial T-cell growth factor (Boyman and Sprent 2012). However, it remains to be studied weather CNFs exert this effect directly, by acting on T-cells, or indirectly, through accessory cells.

We believe that the down-regulating effect of CNFs on T-cell activation is predominantly mediated by accessory cells, as these cells are the first immune cells that come into contact with foreign materials. CNFs are micron in length and thus hardly phagocytable by monocytes/macrophages and dendritic cells. Dong et al. (2012) showed that the uptake of CNCs by both phagocytic and non-phagocytic cells, which are much smaller in diameter and shorter in length than CNFs, was minimal at less than 3 and 1 %, respectively. Such phenomenon might be due to repulsive forces between the negatively-charged nanocrystals and cell membrane. Other authors (Clift et al. 2011) have demonstrated that cotton-derived CNCs enter the phagocytic cells through a form of endocytosis and upon internalisation the nanofibers are localised within endosomal vesicles. Whether some small fragments of CNFs, that can be formed during the preparation and ultrasonic treatment of CNFs, use the same pathway to enter the phagocytic cells remains to be studied. It is less likely that CNFs cause a form of frustrated phagocytosis, which is typical for crocidolite asbestos fibres (Clift et al. 2011), but rather the nanofibrils interact with cell receptors on immune cells by mechanisms that are as yet unexplored.

We believe that the contacts of CNFs with membranous receptors on immune cells are of crucial importance for immunomodulation. In this context, it is worth mentioning that our culture model is not quite suitable for adherent cells such as L929 cells due to the formation of floating CNF aggregates. The reason for that could be the presence of not fully dissociated weak carboxylic ($–COO^-$) acids groups on nanofibrils, terminally located. However, when using cell suspension cultures such as PHA-stimulated PBMNC clusters or dendritic cells (the study in progress), a much higher quantity of CNFs interacted with the cells and the contacts were more visible when the samples were stained with Calcofluor white (data not shown). Calcofluor white is a fluorescence dye that stains cellulose and chitin fibres and is used in microbiology for identifying fungi in biological samples. This dye has been used for the first time in this work for staining CNFs and we found that this is an excellent tool for the microscopic examinations and characterisations of CNFs.

Unchanged production of TNF-α and IL-1β, two of the main pro-inflammatory cytokines produced predominantly by phagocytic cells upon phagocytosis/endocytosis of foreign materials, favours the hypothesis that CNFs do not enter phagocytes. These findings are in accordance with those published by Vartiainen et al. (2011) who demonstrated that microfibrillated cellulose did not caused any effects on TNF-α and IL-1β expression in a mouse monocytic cell line (RAW 264.7 cells) and human monocyte derived macrophages. In addition, it has

been shown that microfibrillated nanocellulose was unable to trigger the production of TNF-α by human macrophage-like THP-1 cells, nor to modify the lipopolysaccharide (LPS)-induced production of TNF-α (Kollar et al. 2011), in contrast to microcrystalline nanocellulose, which significantly blocked the LPS-stimulated TNF-α secretion. Although our study should be extended to examine the effect of CNFs on the production of pro-inflammatory cytokines by isolated macrophages and dendritic cells, the findings that the secretion of both TNF-α and IL-1β in PBMNC cultures was unchanged by CNFs indicate that this wood-derived nanocellulose did not trigger the inflammatory response. This is very important if CNFs could be used for promoting wound healing (Ryšavá et al. 2003), where the inflammatory type of macrophages should be silenced (Adamson 2009).

We showed for the first time the ability of CNFs to modulate the immune responses of Th cells in vitro by modulating the production of Th cytokines. It is known that upon antigenic stimulation, which was mimicked in our study by polyclonal T-cell stimulation in the presence of PHA, $CD4^+$ T-cells can be polarised to various effector subsets, each of them characterised by the production of subset- specific cytokines. Four Th subsets (Th1, Th2, Th17 and Tregs) are well characterized in terms of their phenotypic properties and functions (Zhu et al. 2010). Th1 cells, by producing IFN-γ, are key players in the eradication of intracellular infections. Th2 cells, which produce IL-4, IL-5 and IL-13, are involved in anti-helmintic infections and allergy diseases. Th17 cells produce IL-17 and IL-22 cytokines, and from amongst them IL-17A is the more important for immunity against extracellular bacteria and fungi. Th1 and Th17 cells have been thought to be responsible for many autoimmune diseases by promoting different inflammatory reactions. Tregs cytokines, particularly IL-10 and TGF-β, are immunomodulary cytokines responsible for down-regulation of the immune response and the induction of tolerance both to self and foreign antigens (Long and Buckner 2011; Ouyang et al. 2011).

We showed that CNFs inhibited Th1 and Th17 responses as estimated by decreased production of IFN-γ and IL-17A by PHA-stimulated lymphocytes, respectively. The inhibition of IFN-γ was stronger than IL-17A. As both cytokines exert the pro-inflammatory activity, our findings may be relevant for using CNFs as an anti-inflammatory biomaterial. Such properties could be additionally potentiated by increased production of IL-10, the key anti-inflammatory and immunoregulatory cytokine. IL-10 is produced by various cell subsets, including Tregs and phagocytic cells (Ouyang et al. 2011). Our previous paper showed that gold nanoparticles acted down-modulatory on the immune response by increasing the production of IL-10 and subsequent down-regulation of IL-12 and IL-23 by dendritic cells (Tomic et al. 2014), which are Th1- and Th17-inducing cytokines, respectively (Čolić et al. 2009; Zhu et al. 2010). Such mechanisms may also be involved in tolerance induction by CNFs, which is the aim of our ongoing study. Based on all these findings it can be postulated that the effect of CNFs on the immune response is associated primarily with tolerance induction by activating Tregs and the production of immunoregulatory cytokines. IL-6, a pro- and anti-inflammatory cytokine (Wolf et al. 2014), which was also up-regulated by CNFs, may act synergistically with IL-10 in immunoregulation.

In conclusion, our results suggest that wood-based nanofibrillated cellulose can be considered as a cytocompatible material with tolerogenic potential on the immune system. Both properties are very desirable for the clinical application of nanocellulose. It remains to study the mechanisms involved in these immunoregulatory processes in more detail, by focusing on antigen-presenting cells.

Acknowledgments This work was supported by the project MNT-Era-Net n-POSSCOG (Slovenian Ministry of Education, Science, Culture and Sport), and the project ON175102 (Ministry of Education, Science and Technological Development of R. Serbia). The authors thank Sergej Tomic, Jelena Djokic and Milan Markovic for technical support.

References

Adamson R (2009) Role of macrophages in normal wound healing: an overview. J Wound Care 18:349–351

Alexandrescu L, Syverud K, Gatti A, Chinga-Carrasco G (2013) Cytotoxicity tests of cellulose nanofibril-based structures. Cellulose 20:1765–1775

Backdahl H, Helenius G, Bodin A, Nannmark U, Johansson BR, Risberg B, Gatenholm P (2006) Mechanical properties of bacterial cellulose and interactions with smooth muscle cells. Biomaterials 27:2141–2149

Bhattacharya M, Malinen MM, Lauren P, Lou YR, Kuisma SW, Kanninen L, Lille M, Corlu A, GuGuen-Guillouzo C, Ikkala O, Laukkanen A, Urtti A, Yliperttula M (2012)

Nanofibrillar cellulose hydrogel promotes three-dimensional liver cell culture. J Control Release 164:291–298
Boyman O, Sprent J (2012) The role of interleukin-2 during homeostasis and activation of the immune system. Nat Rev Immunol 12:180–190
Chen Y, Junger WG (2012) Measurement of oxidative burst in neutrophils. Methods Mol Biol 844:115–124
Clift MJ, Foster EJ, Vanhecke D, Studer D, Wick P, Gehr P, Rothen-Rutishauser B, Weder C (2011) Investigating the interaction of cellulose nanofibers derived from cotton with a sophisticated 3D human lung cell coculture. Biomacromolecules 12:3666–3673
Colic M, Gasic S, Vucevic D, Pavicic L, Popovic P, Jandric D, Medic-Mijacevic L, Rakic L (2000) Modulatory effect of 7-thia-8-oxoguanosine on proliferation of rat thymocytes in vitro stimulated with concanavalin A. Int J Immunopharmacol 22:203–212
Čolić M, Gazivoda D, Vučević D, Vasilijić S, Rudolf R, Lukić A (2009) Proinflammatory and immunoregulatory mechanisms in periapical lesions. Mol Immunol 47:101–113
Čolić M, Rudolf R, Stamenković D, Anžel I, Vučević D, Jenko M, Lazić V, Lojen G (2010) Relationship between microstructure, cytotoxicity and corrosion properties of a Cu–Al–Ni shape memory alloy. Acta Biomater 6:308–317
Deng DX, Cai L, Chakrabarti S, Cherian MG (1999) Increased radiation-induced apoptosis in mouse thymus in the absence of metallothionein. Toxicology 134:39–49
Dong S, Hirani AA, Colacino KR, Lee YW, Roman M (2012) Cytotoxicity and cellular uptake of cellulose nanocrystals. Nano Life 02:1241006
Dugan JM, Gough JE, Eichhorn SJ (2013) Bacterial cellulose scaffolds and cellulose nanowhiskers for tissue engineering. Nanomedicine 8:287–298
Ferraz N, Carlsson DO, Hong J, Larsson R, Fellstrom B, Nyholm L, Stromme M, Mihranyan A (2012) Haemocompatibility and ion exchange capability of nanocellulose polypyrrole membranes intended for blood purification. J R Soc Interface R Soc 9:1943–1955
Ferraz N, Leschinskaya A, Toomadj F, Fellström B, Strømme M, Mihranyan A (2013) Membrane characterization and solute diffusion in porous composite nanocellulose membranes for hemodialysis. Cellulose 20:2959–2970
Habibi Y (2014) Key advances in the chemical modification of nanocelluloses. Chem Soc Rev 43:1519–1542
Hua K, Carlsson DO, Ålander E, Lindström T, Strømme M, Mihranyan A, Ferraz N (2014) Translational study between structure and biological response of nanocellulose from wood and green algae. RSC Adv 4:2892
ISO10993-5 (2009) Biological evaluation of medical devices. Part 5. Test for *in vitro* cytotoxicity
Jia B, Li Y, Yang B, Xiao D, Zhang S, Rajulu AV, Kondo T, Zhang L, Zhou J (2013) Effect of microcrystal cellulose and cellulose whisker on biocompatibility of cellulose-based electrospun scaffolds. Cellulose 20:1911–1923
Jonoobi M, Aitomäki Y, Mathew AP, Oksman K (2014) Thermoplastic polymer impregnation of cellulose nanofibre networks: morphology, mechanical and optical properties. Compos A 58:30–35
Kalia S, Boufi S, Celli A, Kango S (2013) Nanofibrillated cellulose: surface modification and potential applications. Colloid Polym Sci 292:5–31
Kolakovic R, Peltonen L, Laukkanen A, Hirvonen J, Laaksonen T (2012) Nanofibrillar cellulose films for controlled drug delivery. Eur J Pharm Biopharm 82:308–315
Kollar P, Zavalova V, Hosek J, Havelka P, Sopuch T, Karpisek M, Tretinova D, Suchy P Jr (2011) Cytotoxicity and effects on inflammatory response of modified types of cellulose in macrophage-like THP-1 cells. Int Immunopharmacol 11:997–1001
Lin N, Dufresne A (2014) Nanocellulose in biomedicine: current status and future prospect. Eur Polym J 59:302–325
Liu K, Lin X, Chen L, Huang L, Cao S (2014) Dual-functional chitosan–methylisothiazolinone/microfibrillated cellulose biocomposites for enhancing antibacterial and mechanical properties of agar films. Cellulose 21:519–528
Long SA, Buckner JH (2011) CD4+FOXP3+ T regulatory cells in human autoimmunity: more than a numbers game. J Immunol 187:2061–2066
Lou YR, Kanninen L, Kuisma T, Niklander J, Noon LA, Burks D, Urtti A, Yliperttula M (2014) The use of nanofibrillar cellulose hydrogel as a flexible three-dimensional model to culture human pluripotent stem cells. Stem Cells Dev 23:380–392
Martins NCT, Freire CSR, Pinto RJB, Fernandes SCM, Neto CP, Silvestre AJD, Causio J, Baldi G, Sadocco P, Trindade T (2012) Electrostatic assembly of Ag nanoparticles onto nanofibrillated cellulose for antibacterial paper products. Cellulose 19:1425–1436
Mathew AP, Oksman K, Pierron D, Harmad M-F (2011) Crosslinked fibrous composites based on cellulose nanofibers and collagen with in situ pH induced fibrillation. Cellulose 19:139–150
Mathew AP, Oksman K, Pierron D, Harmand M-F (2012) Fibrous cellulose nanocomposite scaffolds prepared by partial dissolution for potential use as ligament or tendon substitutes. Carbohydr Polym 87:2291–2298
Mathew AP, Oksman K, Pierron D, Harmand MF (2013) Biocompatible fibrous networks of cellulose nanofibres and collagen crosslinked using genipin: potential as artificial ligament/tendons. Macromol Biosci 13:289–298
Mihajlovic D, Vucevic D, Chinou I, Colic M (2014) Royal jelly fatty acids modulate proliferation and cytokine production by human peripheral blood mononuclear cells. Eur Food Res Technol 238:881–887
Miyamoto T, Takahashi S, Ito H, Inagaki H, Noishiki Y (1989) Tissue biocompatibility of cellulose and its derivatives. J Biomed Mater Res 23:125–133
Monopoli MP, Walczyk D, Campbell A, Elia G, Lynch I, Bombelli FB, Dawson KA (2011) Physical–chemical aspects of protein corona: relevance to in vitro and in vivo biological impacts of nanoparticles. J Am Chem Soc 133:2525–2534
Moreira S, Silva NB, Almeida-Lima J, Rocha HAO, Medeiros SRB, Alves C, Gama FM (2009) BC nanofibres: in vitro study of genotoxicity and cell proliferation. Toxicol Lett 189:235–241
Muhle H, Ernst H, Bellmann B (1997) Investigation of the durability of cellulose fibres in rat lungs. Ann Occup Hyg 41(Supplement 1):184–188
O'Flynn K, Krensky AM, Beverley PC, Burakoff SJ, Linch DC (1985) Phytohaemagglutinin activation of T cells through the sheep red blood cell receptor. Nature 313:686–687

Ouyang W, Rutz S, Crellin NK, Valdez PA, Hymowitz SG (2011) Regulation and functions of the IL-10 family of cytokines in inflammation and disease. Annu Rev Immunol 29:71–109

Pereira MM, Raposo NR, Brayner R, Teixeira EM, Oliveira V, Quintao CC, Camargo LS, Mattoso LH, Brandao HM (2013) Cytotoxicity and expression of genes involved in the cellular stress response and apoptosis in mammalian fibroblast exposed to cotton cellulose nanofibers. Nanotechnology 24:075103

Pitkänen M, Kangas H, Laitinen O, Sneck A, Lahtinen P, Peresin MS, Niinimäki J (2014) Characteristics and safety of nano-sized cellulose fibrils. Cellulose 21:3871–3886

Rahman I, Kode A, Biswas SK (2007) Assay for quantitative determination of glutathione and glutathione disulfide levels using enzymatic recycling method. Nat Protoc 1:3159–3165

Ryšavá J, Dyr JE, Homola J, Dostálek J, Křížová P, Mášová L, Suttnar J, Briestenský J, Santar I, Myška K, Pecka M (2003) Surface interactions of oxidized cellulose with fibrin(ogen) and blood platelets. Sens Actuators B 90:243–249

Tada H, Shiho O, Kuroshima K-I, Koyama M, Tsukamoto K (1986) An improved colorimetric assay for interleukin 2. J Immunol Methods 93:157–165

Tatrai E, Brozik M, Adamis Z, Meretey K, Ungvary G (1996) In vivo pulmonary toxicity of cellulose in rats. J Appl Toxicol 16:129–135

Tomic S, Dokic J, Vasilijic S, Ogrinc N, Rudolf R, Pelicon P, Vucevic D, Milosavljevic P, Jankovic S, Anzel I, Rajkovic J, Rupnik MS, Friedrich B, Colic M (2014) Size-dependent effects of gold nanoparticles uptake on maturation and antitumor functions of human dendritic cells in vitro. PLoS One 9:e96584

Valo H, Kovalainen M, Laaksonen P, Hakkinen M, Auriola S, Peltonen L, Linder M, Jarvinen K, Hirvonen J, Laaksonen T (2011) Immobilization of protein-coated drug nanoparticles in nanofibrillar cellulose matrices—enhanced stability and release. J Control Release 156:390–397

Vartiainen J, Pöhler T, Sirola K, Pylkkänen L, Alenius H, Hokkinen J, Tapper U, Lahtinen P, Kapanen A, Putkisto K, Hiekkataipale P, Eronen P, Ruokolainen J, Laukkanen A (2011) Health and environmental safety aspects of friction grinding and spray drying of microfibrillated cellulose. Cellulose 18:775–786

Wolf J, Rose-John S, Garbers C (2014) Interleukin-6 and its receptors: a highly regulated and dynamic system. Cytokine 70:11–20

Yanamala N, Farcas MT, Hatfield MK, Kisin ER, Kagan VE, Geraci CL, Shvedova AA (2014) In vivo evaluation of the pulmonary toxicity of cellulose nanocrystals: a renewable and sustainable nanomaterial of the future. ACS Sustain Chem Eng 2:1691–1698

Zhu J, Yamane H, Paul WE (2010) Differentiation of effector CD4 T cell populations (*). Annu Rev Immunol 28:445–489